

# Higher Alcohols from Synthesis Gas Using Carbon-Supported Doped Molybdenum-Based Catalysts

Xianguo Li,<sup>†</sup> Lijuan Feng,<sup>†</sup> Zhenyu Liu,<sup>‡</sup> Bing Zhong,<sup>‡</sup> Dady B. Dadyburjor,\* and Edwin L. Kugler

Department of Chemical Engineering, West Virginia University, P.O. Box 6102, Morgantown, West Virginia 26506-6102

A series of carbon-supported molybdenum-based catalysts was prepared by incipient wetness impregnation. The materials, when promoted with potassium and additionally with cobalt, were screened for the selective production of mixed higher-molecular-weight alcohols from syngas. The effects of the catalyst preparation parameters (Mo precursor, Mo loading, doping levels of K and Co, and calcination) and of the reaction conditions (temperature and space velocity) were studied. The screening procedure consisted of ramping the temperature steadily from 200 to 400 °C and back again. Adding K results in a maximum in the space–time yield (STY) of total alcohols and the ratio of higher alcohols to methanol. Increasing the reaction temperature results in a monotonic increase in the STY of hydrocarbons, a monotonic decrease in the selectivity toward alcohols, and a maximum in the STY of alcohols. Increasing the space velocity increases the STY and selectivity to alcohols while decreasing the STY of hydrocarbons. Increasing the space velocity also decreases the higher-alcohol fraction in the alcohol products.

## Introduction

Over the past decade or so, the synthesis of mixed alcohols has drawn considerable interest due to the increasing demand for octane boosters. The incentive stems from the phasing out of lead from the gasoline pool by legislation and the reduction of volatile compounds. Higher alcohols (ethanol and those of higher molecular weight) are preferable to methanol because of their lower volatility and higher solubility in hydrocarbons.

It is widely recognized that higher alcohols together with methanol (MeOH) can be produced from syngas, a mixture of carbon monoxide and hydrogen, by appropriate modification of MeOH-synthesis catalysts and the reaction conditions.<sup>1,2</sup> Italian researchers<sup>3–7</sup> have worked extensively with Cu- and Zn-based oxide catalysts, especially those with spinel-like structures, although their performance for alcohol synthesis has not been so good. The Lehigh group<sup>8–11</sup> has emphasized the direct synthesis of isobutanol over Cu-based catalysts. These researchers have found that Cs doping significantly enhances the selectivity and productivity to isobutanol and have studied the mechanisms and kinetics of alcohol formation over these catalysts.

Other catalyst types have also been used for the synthesis of higher alcohols. In the 1980s, Rh- and Ru-based catalysts were explored<sup>12,13</sup> for the synthesis of higher oxygenates. Classical Fischer–Tropsch (F–T) catalysts have also been modified, by addition of alkali

metals or by nitridation, to improve the selectivity toward alcohols.<sup>14</sup> The Institut Francais du Petrole has claimed that mixtures of light alcohols could be produced over a series of catalysts consisting of MeOH synthesis catalysts and F–T catalysts.<sup>15</sup>

The final category of catalysts for the synthesis of higher alcohols is promoted Mo-based materials, which is the focus of the present work. Research groups at Dow Chemical<sup>16,17</sup> and Union Carbide<sup>18</sup> discovered that molybdenum sulfide catalysts promoted by cobalt or/and alkali-metal compounds are active for the production of C<sub>1</sub>–C<sub>5</sub> alcohols. Xie et al.<sup>19</sup> have reported the effect of pressure on alcohol synthesis over K<sub>2</sub>CO<sub>3</sub>-promoted MoS<sub>2</sub> catalysts prepared by thermolysis of ammonium tetrathiomolybdate. The Lehigh research group has worked extensively with alkali-metal-doped unsupported MoS<sub>2</sub> catalysts as well, with special emphasis on the effect of promoters.<sup>20</sup> Tatsumi et al.<sup>21</sup> reported the effect of potassium promoter on alcohol synthesis over reduced oxide-supported molybdenum catalysts. The role of the alkali-metal promoter has also been studied by Jiang et al.<sup>22</sup> and by Lee et al.<sup>23</sup>

Most of the previous work on molybdenum-based catalysts used for alcohol synthesis deals with unsupported materials with alkali-metal promoters. It is reasonable to expect that the catalytic performance on supported catalysts would be different from that on unsupported ones. It is also expected that the catalytic performance depends, to a certain extent, on the support used. Carbon-supported catalysts have been claimed to have some potential advantages over oxide-supported ones, such as lower tendencies of carbon deposition<sup>24</sup> and less dehydration. In the present work, we prepared a series of activated carbon-supported molybdenum-based catalysts by incipient wetness impregnation. The materials were then used as catalysts for the synthesis of mixed alcohols. The effects of the catalyst preparation parameters and reaction conditions on the catalytic

\* To whom correspondence should be addressed: Telephone: (304) 293-2111, ext. 411. Fax: (304) 293-4139. E-mail: dadyburjor@cemr.wvu.edu.

<sup>†</sup> Current address: College of Chemistry and Chemical Engineering, Ocean University of Qingdao, Qingdao, Shandong 266003, China.

<sup>‡</sup> Current address: Institute of Coal Chemistry, Chinese Academy of Sciences, P.O. Box 165, Taiyuan, Shanxi 030001, People's Republic of China.

**Table 1.** List of Catalysts Used in This Study

catalyst	designation code	Mo precursor	Mo loading, wt %	K precursor	K/Mo molar ratio	Co/Mo molar ratio	calcination
I	Mo/C	AHM <sup>a</sup>	18	N/A	N/A	N/A	no
II	Mo-K/C	AHM	18	K <sub>2</sub> CO <sub>3</sub>	0.3	N/A	no
III	Mo-K/C	AHM	18	K <sub>2</sub> CO <sub>3</sub>	0.5	N/A	no
IV	Mo-K/C	AHM	18	K <sub>2</sub> CO <sub>3</sub>	0.7	N/A	no
V	Mo-K/C	AHM	18	K <sub>2</sub> CO <sub>3</sub>	1.0	N/A	no
VI	Mo-K/C	AHM	18	K <sub>2</sub> CO <sub>3</sub>	1.3	N/A	no
VII	Mo-K/C	AHM	18	K <sub>2</sub> CO <sub>3</sub>	3.0	N/A	no
VIII	Mo-K/C	AHM	3	K <sub>2</sub> CO <sub>3</sub>	1.0	N/A	no
IX	Mo-K/C	AHM	6	K <sub>2</sub> CO <sub>3</sub>	1.0	N/A	no
X	Mo-Co-K/C	AHM	18	K <sub>2</sub> CO <sub>3</sub>	1.3	0.34	no
XI	K-Mo-Co/C	AHM	18	K <sub>2</sub> CO <sub>3</sub>	1.3	0.34	no
XII	Co-impregnated Mo-Co-K/C	AHM	18	K <sub>2</sub> CO <sub>3</sub>	1.3	0.34	no
XIII	Mo-Co-K/C	Mo(C <sub>2</sub> O <sub>4</sub> ) <sub>3</sub>	18	K <sub>2</sub> CO <sub>3</sub>	1.3	0.34	no
XIV	Mo-Co-K/C	Mo(C <sub>2</sub> O <sub>4</sub> ) <sub>3</sub>	18	K <sub>2</sub> CO <sub>3</sub>	1.3	0.34	yes

<sup>a</sup> AHM, ammonium heptamolybdate, (NH<sub>4</sub>)<sub>6</sub>Mo<sub>7</sub>O<sub>24</sub>·4H<sub>2</sub>O.

performance were studied using a temperature-scanning screening technique as described below.

## Experimental Section

**Chemicals.** The activated carbon used for the catalyst support was obtained from Aldrich Chemical Co. The activated carbon has a granule size of 20–40 mesh, a total BET surface area of 660 m<sup>2</sup>/g, and a total pore volume of 1.00 mL/g. To remove the soluble impurities, the activated carbon was treated in boiling water for 1 h. This was followed by filtering and drying in air at 100 °C for 2 h.

Ammonium heptamolybdate [AHM, (NH<sub>4</sub>)<sub>6</sub>Mo<sub>7</sub>O<sub>24</sub>·4H<sub>2</sub>O], potassium carbonate [K<sub>2</sub>CO<sub>3</sub>], and cobalt nitrate [Co(NO<sub>3</sub>)<sub>2</sub>·6H<sub>2</sub>O] were obtained from Fisher Scientific and were used as received. Oxalic acid [H<sub>2</sub>C<sub>2</sub>O<sub>4</sub>] was from Aldrich and was also used as received. All gases used for the catalyst pretreatment and testing were obtained from Matheson; except for CO, all gases were used as received. The CO was passed through an activated-carbon scrubber to remove metal carbonyls.

**Preparation of the Catalysts.** The incipient-wetness technique was used to prepare the carbon-supported Mo-based catalysts. The “standard” source of Mo was AHM. Generally, Mo was impregnated first onto the carbon support, followed by Co (if applicable), with the alkali metal (K) being the last one to be impregnated. Each impregnation step was usually followed by drying, first in air for 4 h at room temperature and then overnight at about 100 °C. Multiple impregnation steps for one component were needed for the preparation of the catalysts with relatively high metal loadings. In these cases, the drying steps were not carried out between each impregnation step.

For comparison, other procedures were also employed for the preparation of the catalyst. In one, a different impregnation sequence was used: K was impregnated first onto the C support, followed by Mo and Co. In a second alternative procedure, molybdenum oxalate [Mo-(C<sub>2</sub>O<sub>4</sub>)<sub>3</sub>] was used as the Mo precursor instead of ammonium heptamolybdate. The molybdenum oxalate was made by reacting ammonium heptamolybdate with oxalic acid (H<sub>2</sub>C<sub>2</sub>O<sub>4</sub>). In a third alternative, after the impregnation steps were completed, the material was calcined in flowing N<sub>2</sub> at 500 °C for 2 h. In this procedure, the Mo source was also the oxalate. The final alternative was the use of a co-impregnation procedure: the three components (Mo, Co, and K) were added

simultaneously onto the support using a mixed solution. Multiple impregnation steps were used in this procedure.

Table 1 lists all the catalysts used in this study. Note that the sequence of elements in the catalyst designation code represents the sequence of impregnation, with the exception of the co-impregnated catalyst.

**Catalytic Reaction.** The reactor system is shown in Figure 1. Since the apparatus has been described elsewhere in detail,<sup>25</sup> only a brief description is provided here. The unit is designed to operate from atmospheric pressure to 1500 psig and at temperatures up to 500 °C. Almost all operating conditions are set directly from a personal computer (PC), the one exception being the reactor pressure, which must be set manually. Data are logged by the PC at operator-determined intervals. The entire unit is located in a walk-in hood. The PC monitors alarms for CO and H<sub>2</sub>S and, for flows of reactive gases, hood velocity, ambient hood temperature, reactor temperature, reactor pressure, compressed-air supply, and electric power. The unit automatically shuts down in the event of hood failure, fire, power- or air-supply failure, or CO or H<sub>2</sub>S leak detection, or if gas flows or reactor temperatures exceed preset operating ranges.

The unit has four lines for gas feed, each independently controlled, and one line for a liquid feed. (The liquid feed line was not used in this work.) The reactor is a stainless-steel tube placed in a single-zone furnace. Typically, 0.5 g of catalyst and 3 g of crushed quartz are mixed together and placed in the center of the reactor, with Pyrex beads upstream and downstream of the catalyst-quartz mixture. The product stream is sampled immediately downstream of the reactor at the pressure of the reactor and at a minimum temperature of 150 °C. The products are analyzed on-line, using a gas chromatograph (GC) containing two columns and two detectors in parallel. The oven temperature for both columns is programmed from 40 to 240 °C. The packed column is connected to a thermal conductivity detector (TCD) which provides quantitative analysis for N<sub>2</sub> (an internal standard) as well as for CO, CO<sub>2</sub>, and H<sub>2</sub>O; H<sub>2</sub> is separated but cannot be measured satisfactorily. The capillary column is connected to a flame-ionization detector (FID), separates all of the C<sub>1</sub>–C<sub>5</sub> alcohols, and separates the C<sub>1</sub>–C<sub>6</sub> hydrocarbons as a single peak. The reactor effluent that is not passed through the GC is

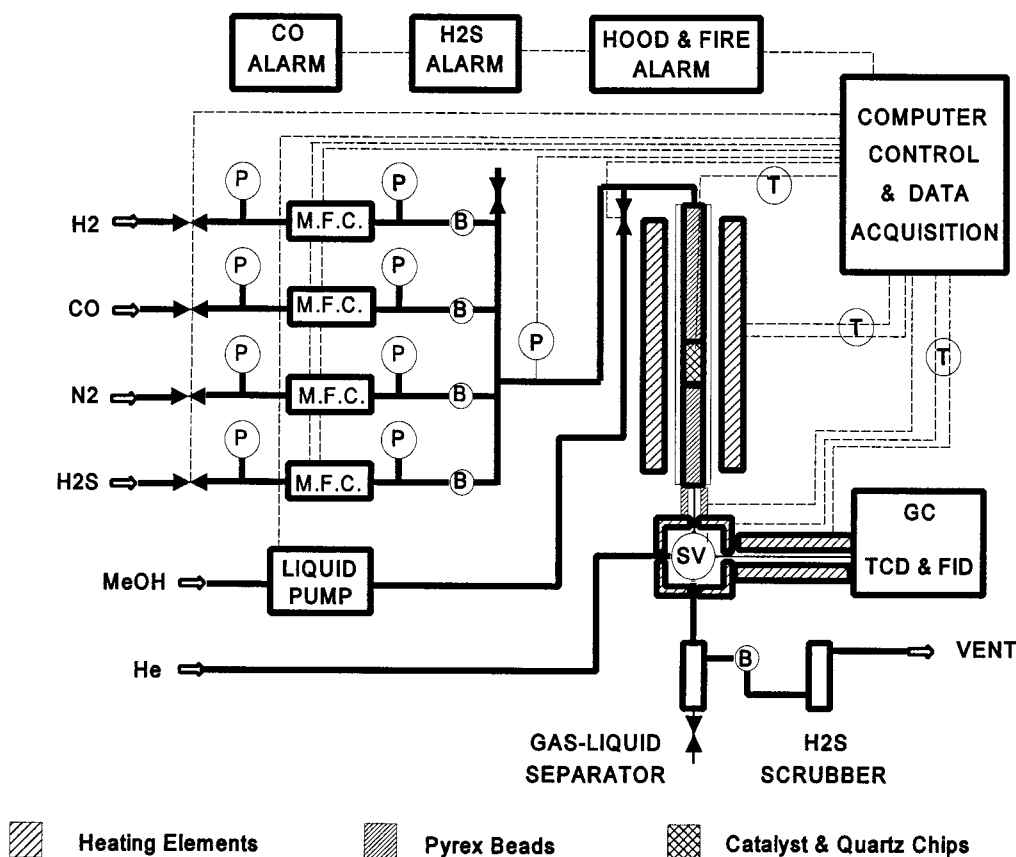


**Figure 1.** Schematic representation of the reactor system. B, back-pressure regulator; MFC, mass-flow controller; P, pressure gauge; SV, sample valve; T, thermocouple.

separated by phase. The liquid phase is collected and the vapor phase is vented after passing through an H<sub>2</sub>S scrubber.

Prior to reaction, the catalyst was first presulfided in situ in a flowing mixture of 10% H<sub>2</sub>S in H<sub>2</sub> (50 cm<sup>3</sup>/min for 0.5 g of catalyst) at 400 °C and atmospheric pressure for 1 h, followed by purging in H<sub>2</sub> (50 cm<sup>3</sup>/min) at the same temperature for 0.5 h. After this pretreatment procedure, the temperature was lowered to about 190 °C (slightly lower than the starting value of the temperature scan), and the system was then pressurized to the desired value, normally 750 psig. Finally, the gas flows were adjusted to the preset values, typically 25 cm<sup>3</sup>(STP)/min for H<sub>2</sub> and 25 cm<sup>3</sup>(STP)/min for CO. This corresponds to a gas-hourly space velocity of 6 m<sup>3</sup>(STP)/h/kg of catalyst.

The reactions were carried out in a temperature-ramping process as follows. The pressure was kept constant, usually 750 psig. The temperature was increased linearly from 200 to 400 °C at a steady rate of 10 °C/h. After the temperature reached 400 °C, it was then decreased at the same steady rate until it was 200 °C once again. Some isothermal runs were also carried out. Here the temperature was raised rapidly to the required temperature and maintained at that value. In all cases, the reaction products were sampled every 2 h and were analyzed by the GC.

## Results and Discussion

**Screening of the Catalysts. Preliminaries.** During our screening runs, the reaction temperature was usually cycled from 200 to 400 °C, as described in the Experimental Section. In our previous study,<sup>25</sup> for runs

in which the temperature cycle was repeated, we found that the second cycle most nearly repeated the data obtained from the decreasing-temperature leg of the first cycle. It is therefore reasonable to believe that the decreasing-temperature leg of the first cycle accurately represents the temperature dependence of the catalytic performance. Therefore, only those data from the decreasing-temperature leg are reported and discussed in this paper.

The reactor tube packed with only Pyrex beads (i.e., without any catalyst) was first tested, to determine the reactivity of the stainless steel reactor. From Figure 2, the CO conversion is vanishingly small. Also shown in Figure 2 are values of the space-time yield (STY) for the total hydrocarbons and the total alcohols separately as products. An (dummy) amount of 0.5 g of inert (catalyst) was used to calculate the values of the STYs; this allows a comparison with actual catalytic runs and also allows us to estimate errors for the calculation of the STYs for the actual catalytic runs.

**Mo/C Catalyst.** The performance of the Mo/C catalyst (catalyst I in Table 1) is shown in Figure 3. While the catalyst is clearly very active for CO hydrogenation, the predominant products are light hydrocarbons. Methanol and ethanol are the only two alcohol products observed, and they are present in very small amounts compared to the hydrocarbons. We return to this below. These observations are consistent with earlier results from our laboratory<sup>25</sup> and from other laboratories<sup>16,18–20,29</sup> when unsupported MoS<sub>2</sub> was used.

**Mo–K/C Catalysts.** Figure 4 gives the catalytic performances of the catalysts that have been doped with varying amounts of K. The catalysts labeled I–VII in Table 1 were used in this portion of the work. With

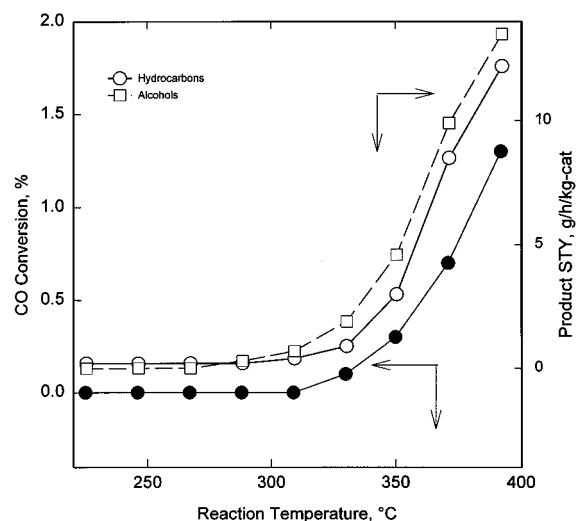


**Figure 2.** Reactivity of the reactor tube packed with Pyrex beads. Reaction conditions:  $P = 750$  psig, flow rate of  $H_2$  and  $CO = 25$   $cm^3$  (STP)/min each.

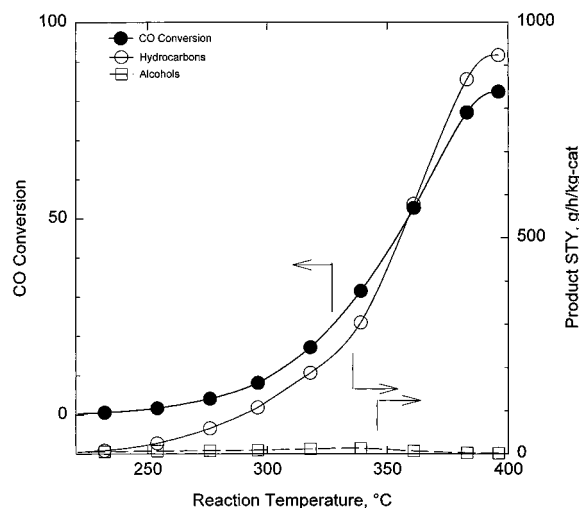


**Figure 3.** Results of the screening run on a Mo/C catalyst with Mo loading of 18 wt %. Reaction conditions: 0.51 g of catalyst; other conditions as in Figure 2. This corresponds to a GHSV of 6  $m^3/h/kg$  of catalyst.

increasing temperature, the following features are typical for all of the K loadings used: a monotonic increase in the overall CO conversion and in the STY of hydrocarbons, a maximum for the STY of the total alcohols, a monotonic increase of  $CO_2$  selectivity with temperature (except perhaps for K/Mo ratios of 0.5–0.7 at low temperatures), a monotonic decline in the  $CO_2$ -free selectivity to total alcohols, and a maximum in the molar ratio of higher alcohols (ethanol and higher) to methanol. (Recall that the decreasing-temperature leg was used to obtain these data.) These results are consistent with those from other laboratories using sulfide catalysts<sup>29</sup> as well as oxide catalysts.<sup>26</sup> It has been postulated that the activation energy for methanol synthesis is lower than that for the formation of hydrocarbons and higher alcohols.

The catalytic performances for different K/Mo molar ratios are also compared in Figure 4. Obviously, K doping causes dramatic changes in the catalytic performance. First, the overall CO conversion decreases significantly upon the first addition of  $K_2CO_3$  into the catalyst (K/Mo = 0.3). Even if the activity is based on the amount of Mo in the catalyst, i.e., if the “specific”

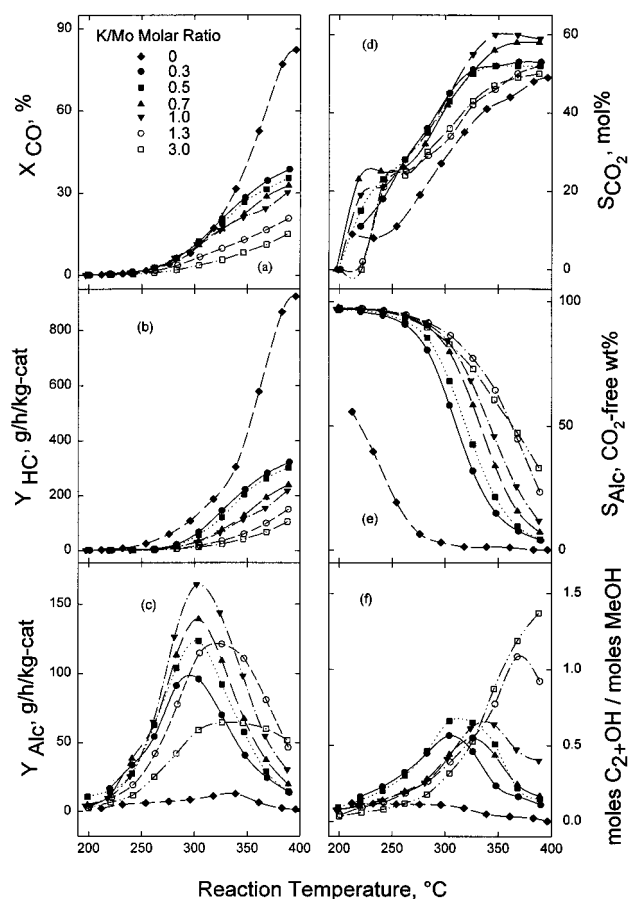


**Figure 4.** Catalytic performances of Mo-K/C catalysts with different K/Mo molar ratios. The following parameters are reported:  $X_{CO}$ , the conversion of CO;  $Y_{HC}$  and  $Y_{Alc}$ , space-time yields of hydrocarbon and total alcohol, respectively;  $S_{CO_2}$  and  $S_{Alc}$ , selectivities of  $CO_2$  and total alcohols ( $CO_2$ -free basis), respectively; and  $C_{2+OH}/MeOH$ , the molar ratio of higher alcohols to methanol. The different catalysts all have the same Mo loading, 18 wt %. Amounts of catalysts used: 0.51 g for catalysts with K/Mo molar ratios of 0 and 0.3; 0.50 g for the remaining catalysts. Other reaction conditions are the same as in Figure 2.

activity is considered, the value still decreases. As the K/Mo ratio increases further, the overall CO conversion keeps decreasing, but proportionately not as much as for the initial addition of K.

Second, the STY of hydrocarbons shows a parallel decline, from about 900 (K/Mo = 0) to around 300 g/h/kg of catalyst (for K/Mo = 0.3) at the highest temperature studied. Again, as the K/Mo ratio increases further, the STYs of hydrocarbons decrease further, but not as dramatically as for the initial addition.

Third, the formation of alcohols is greatly promoted by the K doping. For the undoped catalyst, the STY of total alcohols is essentially zero, if the reactivity of the reactor itself is taken into account. However, for the catalyst with a K/Mo molar ratio of 0.3, the highest STY of total alcohols (at approximately 300 °C) approaches 100 g/h/kg of catalyst. Further, the maximum in the STYs increases with increasing K/Mo, up to values of unity. At higher values, the maximum STY decreases with increasing K/Mo ratio. Finally, the location of the maximum STY seems to be more or less independent of K/Mo for values of the ratio less than or equal to unity. At higher values of K/Mo, the optimum temperature increases slightly, to about 320 °C, but then appears to be unchanged, at least up to values of K/Mo = 3.



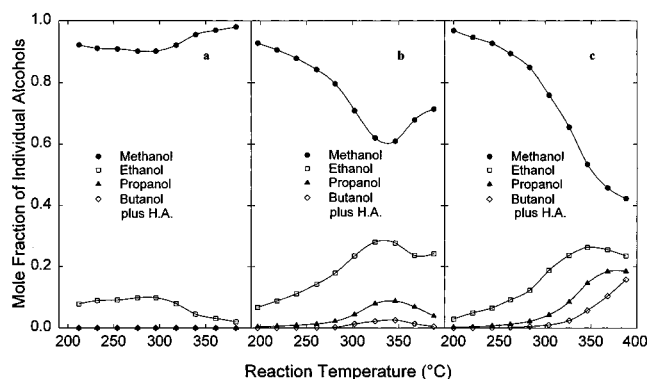


**Figure 5.** Distribution of alcohols formed as functions of temperature over three of the Mo–K/C catalysts used for Figure 4. In all cases, the Mo loading is 18 wt %. K/Mo values are (a) 0, (b) 1.0, and (c) 3.0.

Fourth, the CO<sub>2</sub> molar selectivity increases slightly with the initial addition of K. The molar selectivity toward CO<sub>2</sub> increases further with increasing K/Mo molar ratio up to the value of unity. For dopant values greater than unity, the selectivity decreases with increasing K/Mo.

Finally, as can be seen from Figures 4f and 5, the addition of K<sub>2</sub>CO<sub>3</sub> not only shifts the products toward higher alcohols, it also changes the distribution of alcohols. Figure 4f shows the ratio of higher alcohols to methanol as functions of *T* and K/Mo. At low (but nonzero) values of K/Mo, there is a sharp increase in the molar ratio of higher alcohols at lower temperatures, a maximum value of approximately 0.5 at around 300 °C, and then a falling off. At increasing values of K/Mo, the low-temperature increase is attenuated, the maximum ratio increases, and it occurs at a higher temperature.

Some more insight into this behavior is obtained from Figure 5, in which are plotted the distributions of the individual alcohols for a few values of K/Mo. For the undoped catalyst of Figure 5a, as noted earlier, the absolute amounts of alcohols are low. In fact, only MeOH and EtOH can be detected at all, and the molar distribution of these is probably independent of temperature, within the expected error bars. For large values of K/Mo, of which Figure 5c (with K/Mo = 3) is an example, increasing the temperature leads to a generally monotonically decreasing distribution of MeOH, with successive maxima observed for EtOH, PrOH, and BuOH in turn. However, for intermediate values of K/Mo, of which Figure 5b (with K/Mo = 1) is a typical example, a minimum in the methanol fraction is noted around 350 °C.

It is worth discussing briefly the role of the alkali-metal dopant. Alkali-metal compounds are widely used as promoters in heterogeneous catalysis, particularly for CO hydrogenation. They have been reported either to increase the chain-growth probability or to promote the selective formation of oxygenates in CO hydrogenation. Various, sometimes controversial, explanations have been proposed for the observed effects.<sup>27,28</sup> Klier and co-workers<sup>29</sup> have studied the catalytic performances of CsOOCH-promoted MoS<sub>2</sub> catalysts and suggest that the catalysts are bifunctional: MoS<sub>2</sub> dissociatively activates H<sub>2</sub>, while the alkali-metal component activates CO and decreases the availability of active hydrogen atoms.

For the present catalysts, bifunctionality can also explain the observed promotional effect of K<sub>2</sub>CO<sub>3</sub> toward

the formation of higher alcohols. With increasing K<sub>2</sub>CO<sub>3</sub> levels, the number of CO-activating centers increases, thereby resulting in a greater rate of alcohol formation. When the concentration of K<sub>2</sub>CO<sub>3</sub> exceeds a certain value (K/Mo = 1 in our case), the hydrogenation of the activated intermediates is depressed, due to the decreased availability of active hydrogen atoms, thereby leading to a drop in the STY of total alcohols. That is to say, the balance of the two opposite effects of K<sub>2</sub>CO<sub>3</sub> doping determines the alcohol formation rate.

The decreasing rate of formation of hydrocarbon with the addition of K<sub>2</sub>CO<sub>3</sub> may also be a result of the decreased availability of hydrogenation active centers. For the production of hydrocarbons, the availability of active hydrogen atoms plays a more important role, since the formation of hydrocarbons demands stronger hydrogenation centers. Therefore, it is not surprising that the STY of hydrocarbons decreases monotonically with an increase in the K-doping level.

For classical iron Fischer–Tropsch catalysts, the CO<sub>2</sub> selectivity usually passes through a maximum with increasing alkali-metal concentration.<sup>30</sup> For alkali-metal-promoted MoS<sub>2</sub> catalysts, no one (to our knowledge) has reported the effect of alkali-metal doping on CO<sub>2</sub> selectivity. However, Tatsumi *et al.*<sup>31</sup> report that CO<sub>2</sub> selectivity decreases with an increasing K/Mo molar ratio for mixed-alcohol synthesis over reduced Mo-based catalysts.

As mentioned earlier, alkali-metal promoters act either to increase the chain-growth probability or to promote the formation of oxygenates. Lee *et al.*<sup>23</sup> claim that the two effects are mutually exclusive. But Jiang *et al.*<sup>22</sup> report that alkali-metal compounds not only promote the formation of alcohols but also change the distribution of alcohol products. A maximum in the ratio of higher alcohols to methanol was usually observed with changing alkali-metal concentration. It was also reported<sup>32</sup> that the ratio of higher alcohols to methanol can be adjusted by introducing a sulfur-releasing substance in the feed gas. Our earlier work<sup>25</sup> on alkali-metal-doped MoS<sub>2</sub> prepared by vapor-phase reaction yielded a product distribution consistent with Figure 5c. Such a product distribution can be attributed to a series progression of the formation of the higher alcohols. However, the existence of a minimum in the methanol mole fraction at intermediate values of K/Mo (Figure 5b) is different from that observed earlier. By coupling the data of Figures 5 and 4c, we see that the minimum mole fraction of methanol is not due to an increasing STY of methanol at the highest temperatures. Rather, the methanol STY is decreasing, as are the STYs of the other individual alcohols. This leads us to believe that the increase in the methanol mole fraction is due to a decrease in the formation of higher alcohols from methanol under these conditions and is not due to the existence of an additional pathway for methanol formation from CO and hydrogen. It should be noted that the catalysts used earlier<sup>25</sup> were unsupported or supported on silica, while the catalysts of Figure 5 are supported on activated carbon.

The effect of loading on the performance of the Mo–K/C catalyst is shown in Figure 6. Here the catalysts are doped to the same value of the molar ratio K/Mo, equal to unity, and the amounts of both are increased. The catalysts used are labeled V, VIII, and IX in Table 1. The overall CO conversion increases significantly with increasing loading, as seen in Figure 6a. This

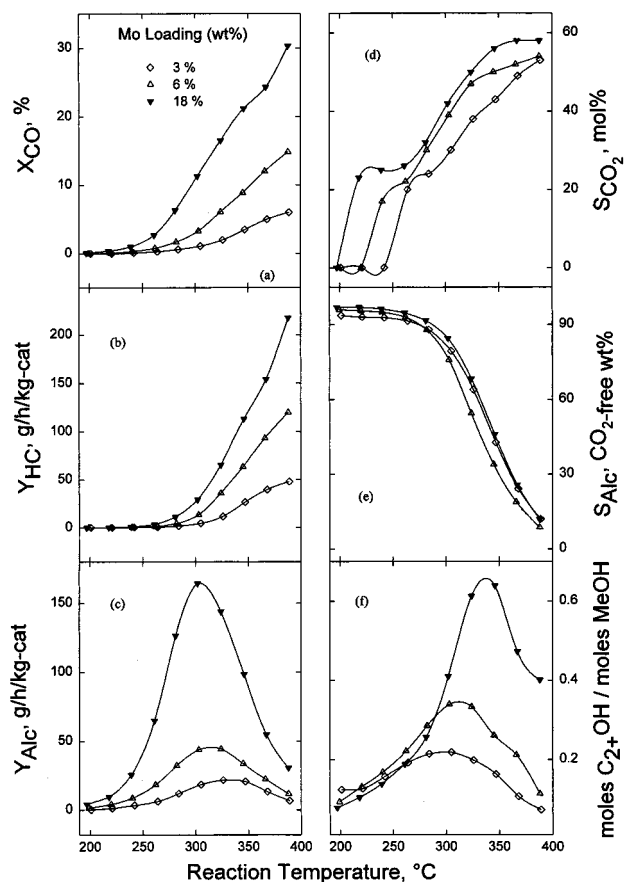


**Figure 6.** Catalytic performances of Mo-K/C catalysts with different Mo loadings. Catalyst parameters are as defined in Figure 4. Each catalyst was doped with K to the same K/Mo molar ratio of unity. In each case, 0.50 g of catalyst was used. Other reaction conditions are as in Figure 2.

indicates an increase of the overall activity and is apparently because of the increase of the concentration of the active component (Mo). Moreover, the STYs of both the total hydrocarbons and the total alcohols increase with increasing Mo content.

Increasing the Mo loading also causes a slight increase in the  $\text{CO}_2$  selectivity. In terms of selectivity toward total alcohols, changing the loading does not cause much difference, as shown in Figure 6e. Clearly, increasing the amount of Mo increases the formation of both hydrocarbons and alcohols in approximately equal amounts. However, increasing the Mo content enhances the relative formation of higher alcohols among the alcohol products, as indicated in Figure 6f. Figure 7 indicates that this change arises as a consequence of the decreasing mole fraction of methanol and the increasing (and no longer negligible) mole fractions of propanol and alcohols of even higher molecular weight.

**Mo-Co-K/C Catalysts.** Figure 8 compares the catalytic performance of a doubly promoted Mo-Co-K/C catalyst (catalyst X in Table 1) with that of a similar catalyst but without Co doping (Mo-K/C, catalyst VI in Table 1). The addition of Co causes a decrease of the overall CO conversion and a decline of the hydrocarbon production rate. The Co causes a shift to the right (higher-temperature) side for the curve for the total alcohol STY so that the STYs decrease at low temperatures but increase at high temperatures: the maximum STY increases, as does the temperature at which the maximum occurs. Also noted is a suppression of

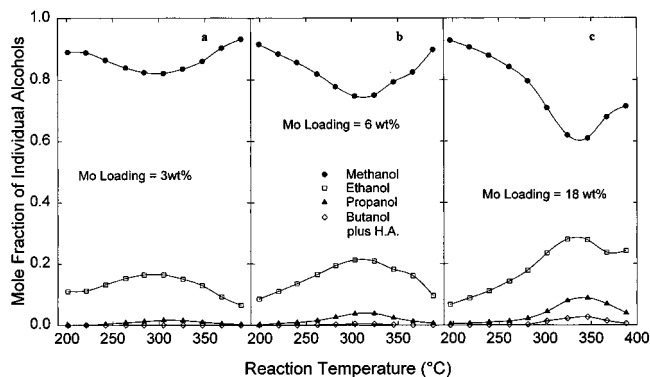


**Figure 7.** Distribution of alcohols formed as functions of temperature over the Mo-K/C catalysts used for Figure 6. In all cases, K/Mo = 1. The Mo loadings are (a) 3, (b) 6, and (c) 18 wt %.

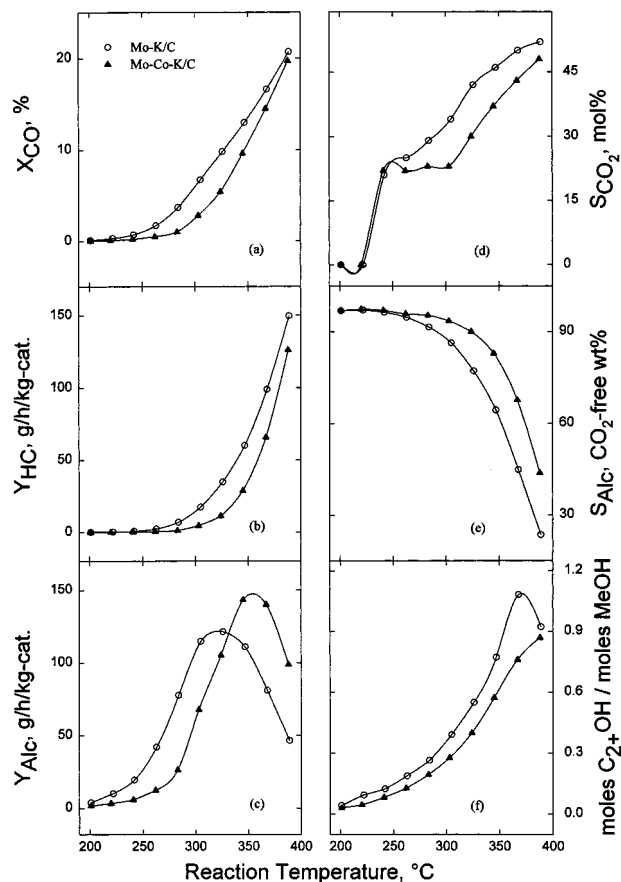


**Figure 8.** Effect of Co doping on catalyst performance. Catalyst parameters are as defined in Figure 4. Both catalysts contain 18 wt % Mo and a molar ratio of K/Mo = 1.33; 0.50 g of catalyst was used for both catalysts. In addition, the Mo-Co-K/C catalyst is doped with Co to a Co/Mo molar ratio of 0.34. Other reaction conditions are as in Figure 2.

$\text{CO}_2$  formation. The selectivity to total alcohols is increased. However, the molar ratio of higher alcohols to methanol decreases. Figure 9 indicates that this decrease is due to a drop in the mole fraction of propanol and other higher-molecular-weight alcohols. Figure 9b also indicates that the presence of Co may remove, or at least diminish, the minimum in the methanol mole fraction at high temperatures.

Stevens<sup>33</sup> disclosed that the preparation method of  $\text{MoS}_2$  catalysts doubly promoted by K and Co may strongly affect the distribution of the alcohol products: co-precipitated Co/Mo sulfide catalysts favor the production of  $\text{C}_2$ - $\text{C}_5$  alcohols, while an impregnated Co- $\text{MoS}_2$

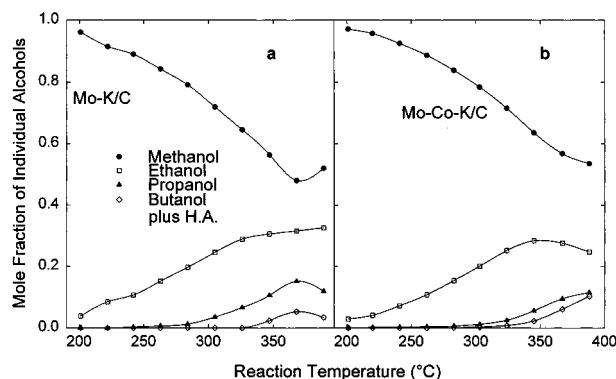


**Figure 9.** Distribution of alcohols formed as functions of temperature over the catalysts used for Figure 8. (a) Mo-K/C; (b) Mo-Co-K/C.

catalyst favors the production of methanol. Further, Murchison *et al.*<sup>34</sup> reported that the addition of Co to an alkali-metal-doped MoS<sub>2</sub> catalyst shifts the selectivity in favor of ethanol. It was postulated that Co promotes the homologation of methanol to form ethanol. Further, the alcohol composition is a strong function of conversion, with higher conversions coinciding with lower methanol contents. However, Murchison *et al.* provided little detail about the preparation of the catalyst. Our result confirms that the addition of Co enhances the formation of higher alcohols while depressing the production of hydrocarbons and CO<sub>2</sub>. Further, the promotional effect of Co is consistent with the observations of Stevens.<sup>33</sup>

It is clearly worth investigating the effect of preparation techniques for the present family of catalysts. Figure 10 summarizes the performances of catalysts X, XI, and XII which were prepared using three different impregnation procedures: Mo first, K first, and co-impregnated, respectively. Note that the three catalysts have the same composition: 18 wt % Mo, K/Mo = 1.3, and Co/Mo = 0.34.

The impregnation sequence Mo-Co-K results in higher activities to both hydrocarbons and alcohols, and a lower CO<sub>2</sub> selectivity, than does the sequence K-Mo-Co. For the co-impregnated catalyst, the overall activity and the activity for hydrocarbon formation are almost the same as those for the impregnation sequence Mo-Co-K. But the co-impregnated catalyst exhibits a higher CO<sub>2</sub> selectivity, thus showing a lower selectivity toward total alcohol formation. In terms of the ratio of higher alcohols to methanol, the co-impregnated catalyst works best at low and medium temperatures. However, the Mo-Co-K sequence may be advantageous at higher temperatures. From Figure 11, the superior performance of the co-impregnated catalyst at the low temperatures can be ascribed to the diminution of the methanol component, especially at low temperatures, while the superior performance of the Mo-Co-K-sequenced catalyst is due to the larger amounts of the butanol-plus compounds. The presence of the cobalt component appears to suppress the minimum in the methanol mole fraction, especially if impregnated last (Figure 11b); however, the co-impregnated catalyst (Figure 11c) exhibits this minimum.

Figure 12 illustrates the effect of the Mo precursor. From this figure, we note that the catalyst from the ammonium molybdate precursor (catalyst X) gives a slightly better performance than does that from the oxalate precursor (catalyst XIII). The distributions of

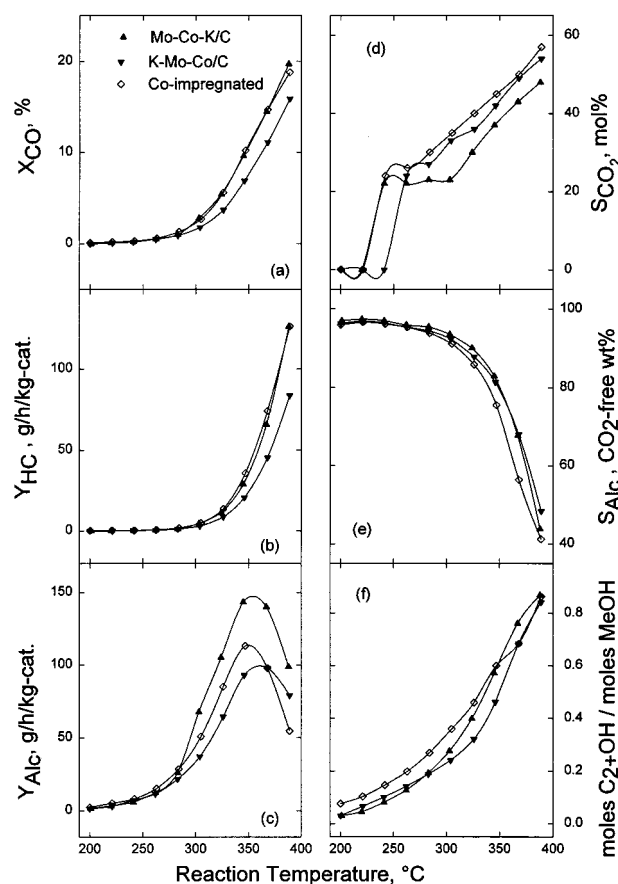


**Figure 10.** Comparison of the catalytic performances of C-supported K- and Co-promoted catalysts prepared using different impregnation procedures. Catalyst parameters are as described in Figure 4. The three catalysts all contain 18 wt % Mo and have the same K/Mo molar ratio of 1.3 and the same Co/Mo molar ratio of 0.34. Amounts of catalysts used: 0.50 g for the Mo-Co-K/C (molybdenum impregnated first) catalyst and for the K-Mo-Co/C (potassium impregnated first) catalyst; 0.51 g for the coimpregnated catalyst. Other reaction conditions are as in Figure 2.

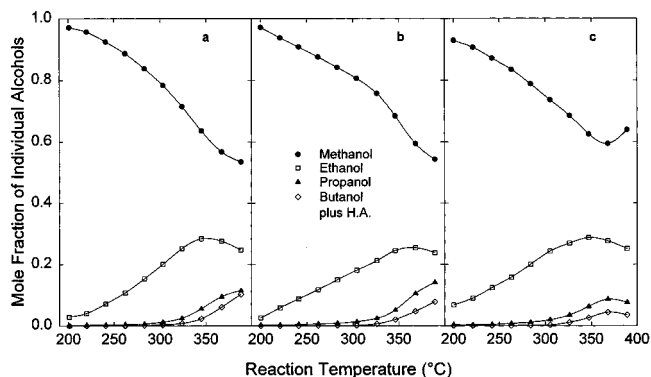


**Figure 11.** Distribution of alcohols formed as functions of temperature over the catalysts used for Figure 10. (a) Mo-Co-K/C; (b) K-Mo-Co/C; (c) coimpregnated catalyst.

the higher alcohols from these two catalysts are not shown, as they are qualitatively similar.

The effect of calcination (in N<sub>2</sub> at 500 °C for 2 h) on the catalytic performance is demonstrated in Figure 13, using catalysts XIII and XIV. Calcination causes a slight increase in the overall CO conversion and an enhancement of hydrocarbon production, both more marked at high temperatures. The STY of total alcohols shifts to the left (lower-temperature) side: the maximum value of the STY is slightly increased, and the

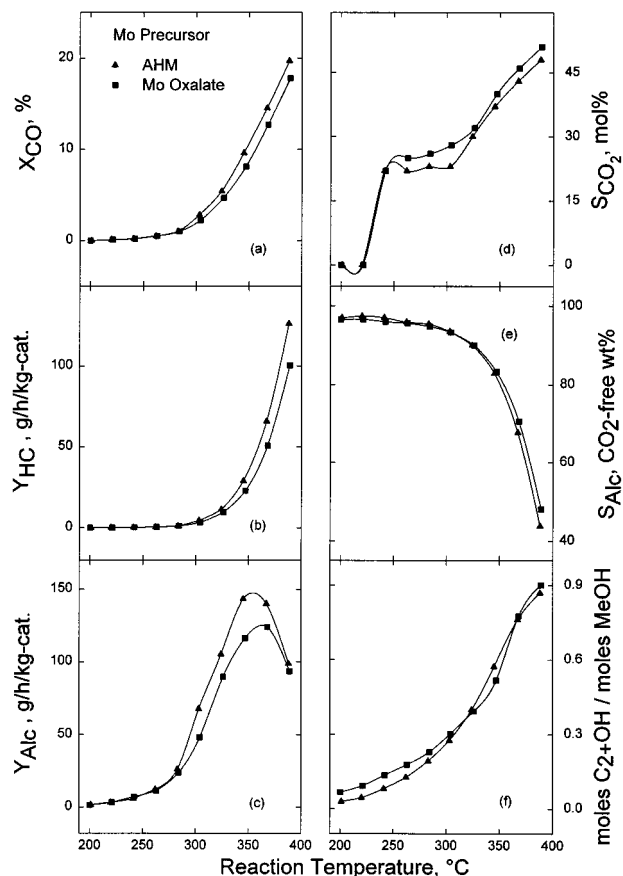


**Figure 12.** Comparison of the catalytic performances of Mo-Co-K/C catalysts prepared from different Mo precursors. Catalyst parameters are as described in Figure 4. The two catalysts have the same composition: Mo loading of 18 wt %, K/Mo molar ratio of 1.3, and Co/Mo molar ratio of 0.34. The same amount of catalyst (0.50 g) was used for the reactions. Other reaction conditions were the same as in Figure 2.

maximum occurs at a slightly lower temperature. Calcination decreases the CO<sub>2</sub>-free selectivity to total alcohols and also decreases the ratio of higher alcohols to methanol. Figure 14 indicates that the decrease in the ratio is due to calcination increasing the methanol mole fraction at the expense of the mole fractions of propanol and higher alcohols. Figure 14 also indicates that calcination results in the reappearance, at high reaction temperatures, of the minimum in the methanol fraction that was removed by the addition of Co.

**Isothermal Performance of a Mo-Co-K/C Catalyst.** The Mo-Co-K/C catalyst performs better than the Mo-K/C or Mo/C catalysts for higher-alcohol synthesis. Therefore, the best Mo-Co-K/C catalyst we have tested (catalyst X in Table 1) was chosen for a series of isothermal runs. Our screening results showed that the catalyst had a maximum STY to total alcohols at temperatures around 350 °C at a space velocity of 6 m<sup>3</sup> (STP)/h/kg of catalyst. Hence, the reaction was carried out isothermally at 350 °C at space velocities of 6, 12, 18, and 21.6 m<sup>3</sup> (STP)/h/kg of catalyst. The results are plotted in Figure 15.

As shown in this figure, higher space velocities result in higher STY values for total alcohols, lower STY values for hydrocarbons, and lower overall CO conversions. In terms of selectivity, a higher space velocity gives a slightly lower CO<sub>2</sub> selectivity, a higher CO<sub>2</sub>-free selectivity to alcohols, but a lower fraction of higher alcohols in the alcohol products. Increasing the space

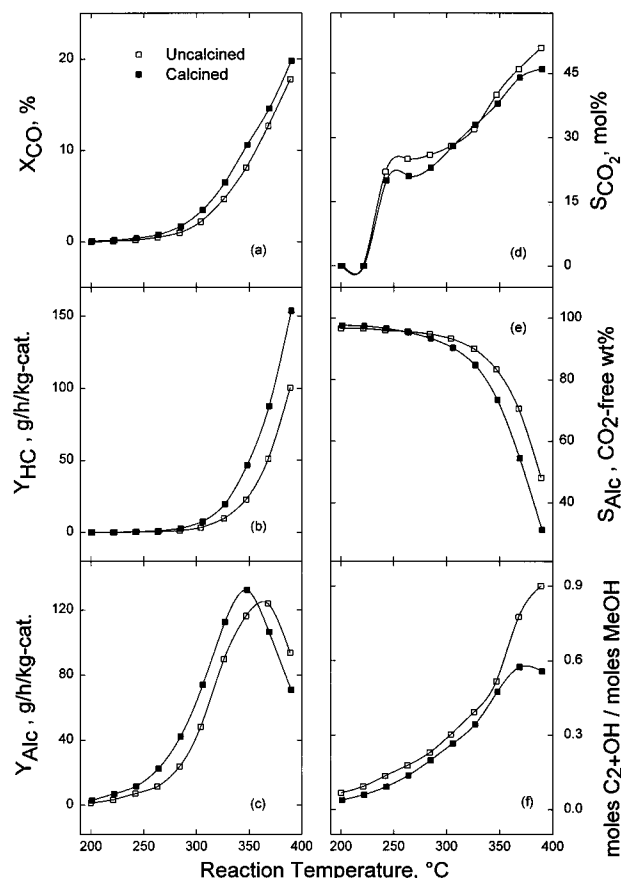


**Figure 13.** Effects of calcination on the performance of the Mo-Co-K/C catalyst. Catalyst parameters are described in Figure 4. The two catalysts have the same composition: Mo loading of 18 wt %, K/Mo molar ratio of 1.3, and Co/Mo molar ratio of 0.34. One catalyst is calcined in flowing N<sub>2</sub> at 500 °C for 2 h, while the other is uncalcined. Amounts of catalysts used: 0.51 g for the calcined catalyst and 0.50 g for the uncalcined catalyst. Other reaction conditions are as in Figure 2.

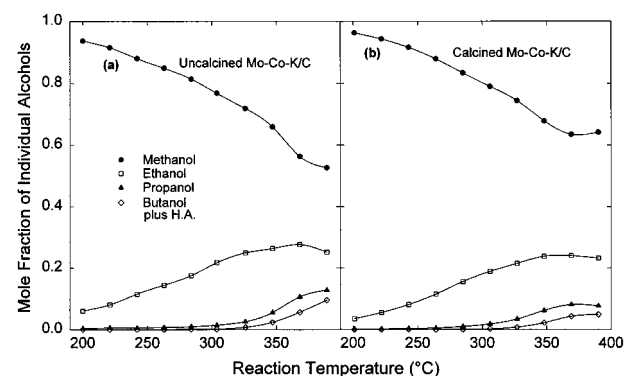


**Figure 14.** Distribution of alcohols formed as functions of temperature over the Mo-Co-K/C catalysts used for Figure 13. (a) Uncalcined catalyst; (b) calcined catalyst.

velocity enhances the production of methanol while suppressing the formation of hydrocarbons and higher alcohols. Since a higher space velocity is associated with a lower residence time, and a lower residence time results in a larger fraction of the primary product and smaller fractions of secondary products, the above results confirm that methanol is a primary product while hydrocarbons and higher alcohols are secondary products. This conclusion is consistent with the theory<sup>29</sup> that higher alcohols are formed by a classical mechanism that proceeds via stepwise CO insertion in alkyl-



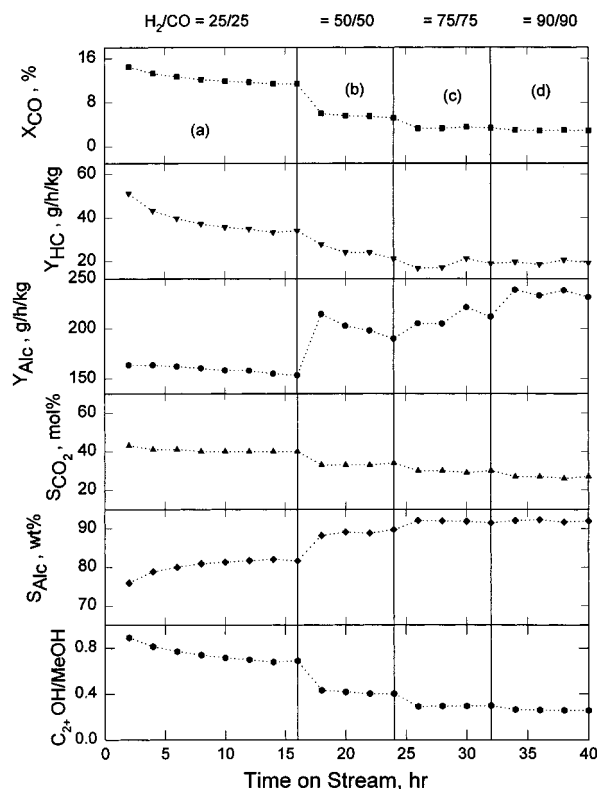


**Figure 15.** Isothermal performances of a Mo-Co-K/C catalyst at 350 °C and 750 psig with increasing GHSV: (a) 6, (b) 12, (c) 18, and (d) 21.6 m<sup>3</sup>/h/kg of catalyst. The corresponding flow rates of H<sub>2</sub> and CO are in units of cm<sup>3</sup> (STP)/min. The catalyst contains 18 wt % Mo and has a K/Mo molar ratio of 1.3 and a Co/Mo molar ratio of 0.34; 0.51 g of catalyst was used. Catalyst parameters are as described in Figure 4.

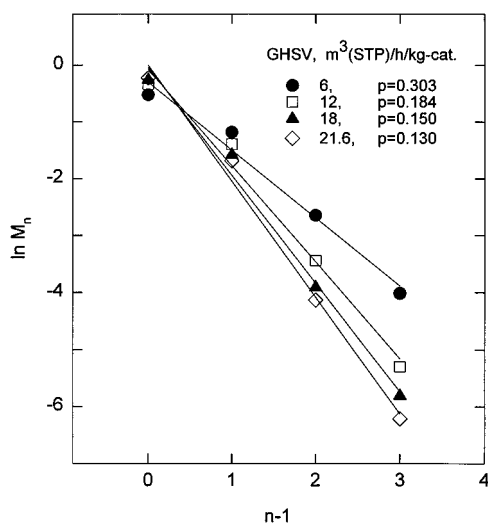


**Figure 16.** Anderson-Schulz-Flory plots for alcohol products at different GHSV values using the catalyst of Figure 15.

metal center bonds and that hydrocarbons are produced by decomposition of alcohols.

The individual distributions of alcohols are depicted in Figure 16, as an Anderson-Schulz-Flory (ASF) plot. Clearly, the carbon-number distributions of the alcohols over the Mo-Co-K/C catalyst follow the ASF distribution. Quantitatively, the ASF distribution can be written as

$$M_n = p^{n-1} (1 - p) \quad (1)$$

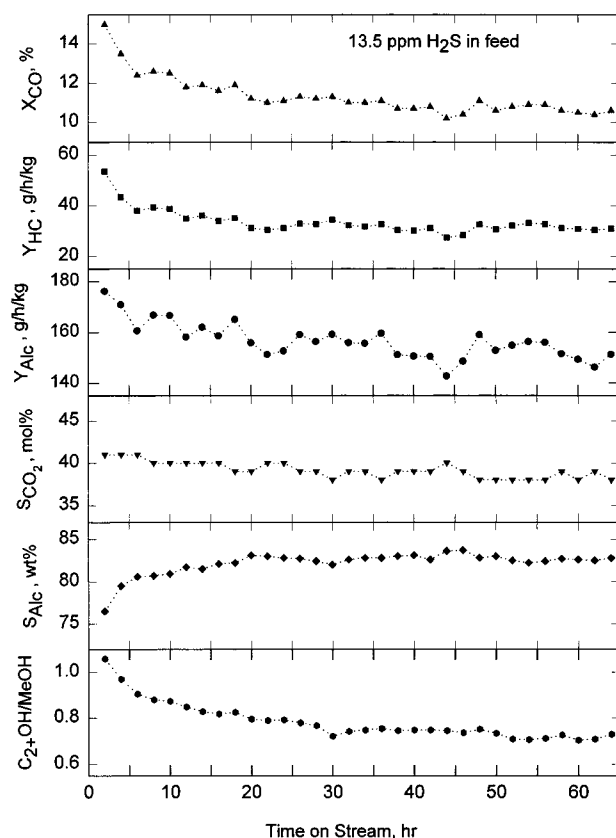


**Figure 17.** Catalytic performance of the catalyst of Figure 15 in a feed containing H<sub>2</sub>S. The sulfur impurity is introduced into the feed for the fresh catalyst and maintained for 65 h. Reaction conditions are as in Figure 15 except that 0.50 g of catalyst is used. Catalyst parameters are as described in Figure 4.

where  $M_n$  is the mole fraction of the product with a carbon number of  $n$  and  $p$  is the chain-growth probability. The values of  $p$ , calculated using the last data point for each space velocity, are shown in Figure 16, along with the corresponding values of the space velocity. The value of the chain-growth probability decreases with increasing space velocity. This is obviously consistent with the product distribution described earlier.

**Effect of Sulfur in the Feed.** Two isothermal runs were carried out with the same Mo-Co-K/C catalyst to evaluate its performance in the presence of H<sub>2</sub>S. In both cases, the reaction temperature was 350 °C, a space velocity of 6 m<sup>3</sup>/h/kg of catalyst was used, and the molar ratio of H<sub>2</sub>/CO in the feed was 1. In one run, 13.5 ppm H<sub>2</sub>S was introduced into the feed at the beginning of the reaction. These results are summarized in Figure 17. For the other run (Figure 18), the same level of impurity, 13.5 ppm H<sub>2</sub>S, was introduced after a reaction time of 16 h. The presence of H<sub>2</sub>S at this level seems to have no effect on the catalytic performance. This is consistent with the known sulfur resistance of molybdenum-sulfide-based catalysts.

## Conclusion

The production of mixed alcohols from synthesis gas (CO and H<sub>2</sub>) was investigated on a series of C-supported Mo-based catalysts. The screening results indicate that carbon-supported sulfided molybdenum promoted by K, optionally promoted by Co, is a suitable material for higher-alcohol synthesis. Calcination of the catalyst has relatively little effect but is not particularly helpful.

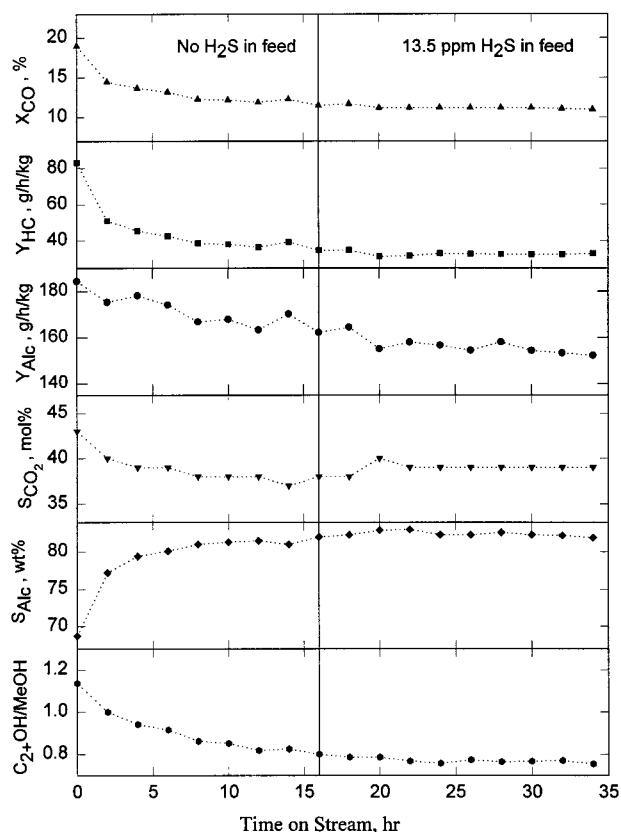


**Figure 18.** Effect of sulfur on the performance of the catalyst of Figure 15. The  $\text{H}_2\text{S}$ -containing feed is now introduced after the catalyst has been on stream for 16 h. Reaction conditions are as in Figure 17. No significant drop in catalyst performance is seen after the introduction of the sulfur impurity. Catalyst parameters are described in Figure 4.

Preparation parameters, such as the type of Mo precursor, the Mo loading, and the K-doping level, affect the catalytic performance to different extents. The catalyst is resistant to sulfur in the feed.

Increasing the space velocity enhances the production of methanol while suppressing the formation of hydrocarbons and higher alcohols. The observations can be well explained by the bifunctionality of the catalyst and by a classical stepwise CO-insertion mechanism. Increasing the reaction temperature increases the selectivity toward hydrocarbons while decreasing the selectivity to alcohols. A maximum in the STY of total alcohols with the reaction temperature is observed for all catalysts tested. The distribution of the individual alcohol products is as follows: increasing temperatures lead to a decreasing mole fraction of methanol and progressive maxima in the mole fractions of higher alcohols. This, too, is consistent with a CO-insertion mechanism. However, at high temperatures, a minimum in the methanol mole fraction is sometimes noted, after which the methanol mole fraction increases with temperature. This implies a decrease in the insertion of CO. The minimum is observed for the case of the C-supported catalyst, small Mo loadings, small levels of K dopings and an absence of Co (or co-impregnation of Co with K and Mo) and if the catalyst is calcined.

The screening results indicate that the catalyst with K/Mo around unity and with Co/Mo around 0.34 is worthy of further study for this process. The typical reaction conditions are expected to be temperatures around  $350^\circ\text{C}$ , pressures around 750 psi,  $\text{CO}/\text{H}_2$  ratios

around unity, and space velocities around  $20\text{ m}^3\text{ (STP)}/\text{h/kg}$  of catalyst. In a separate work,<sup>35</sup> we obtain the reaction kinetics of such a catalyst around these reaction conditions.

## Acknowledgment

This work was supported by the U.S. Department of Energy under Contract No. DE-AC22-91PC91034. We acknowledge Eric Zubovic for his contribution in making some of the catalysts used in this study.

## Literature Cited

- (1) Natta, G.; Colombo, U.; Pasquon, I. Direct Catalytic Synthesis of Higher Alcohols from Carbon Monoxide and Hydrogen. In *Catalysis*; Emmett, P. H., Ed.; Reinhold: New York, 1957; Vol. 5, Chapter 3, p 131.
- (2) Smith, K.; Anderson, R. B. A Chain Growth Scheme for the Higher Alcohols Synthesis. *J. Catal.* **1984**, *85*, 428.
- (3) Villa, P. L.; Forzatti, P.; Buzzi-Ferraris, G.; Garone, G.; Pasquon, I. Synthesis of Alcohols from Carbon Oxides and Hydrogen. I. Kinetics of the Low-Pressure Methanol Synthesis. *Ind. Eng. Chem. Process Des. Dev.* **1985**, *24*, 12.
- (4) Villa, P. L.; Del Piero, G.; Cipelli, A.; Lietti, L.; Pasquon, I. Synthesis of Alcohols from Carbon Oxides and Hydrogen. III. Copper-Manganese-Titanium-Potassium Oxide Systems: Preparation, Characterization of Catalytic Properties. *Appl. Catal.* **1986**, *26*, 161.
- (5) Villa, P. L.; Del Piero, G.; Lietti, L.; Garagiola, F.; Mologni, G.; Tronconi, E.; Pasquon, I. Synthesis of Alcohols from Carbon Oxides and Hydrogen. VI. Zinc and Titanium Oxides: Preparation and Catalytic Activity. *Appl. Catal.* **1987**, *35*, 47.
- (6) Forzatti, P.; Cristiani, C.; Ferlazza, N.; Lietti, L.; Tronconi, E.; Villa, P. L.; Pasquon, I. Synthesis of Alcohols from Carbon Oxides and Hydrogen. VII. Preparation, Activation and Catalytic Behavior of a Zinc-Manganese-Chromium-Potassium Oxide Catalyst. *J. Catal.* **1988**, *111*, 120.
- (7) Forzatti, P.; Tronconi, E.; Pasquon, I. Higher Alcohol Synthesis. *Catal. Rev.-Sci. Eng.* **1991**, *33*, 109.
- (8) Klier, K.; Herman, R. G.; Young, C. W. Direct Synthesis of 2-Methyl-1-Propanol. *Prepr. Pap.-Am. Chem. Soc., Div. Fuel Chem.* **1984**, *29*, 273.
- (9) Nunan, J. G.; Bogdan, C. E.; Klier, K.; Smith, K. J.; Young, C. W.; Herman, R. G. Higher Alcohol and Oxygenate Synthesis over Cesium-Doped Copper/Zinc Oxide Catalysts. *J. Catal.* **1989**, *116*, 195.
- (10) Nunan, J. G.; Herman, R. G.; Klier, K. Higher Alcohol and Oxygenate Synthesis over Cesium/Copper/Zinc Oxide/ $\text{M}_2\text{O}_3$  ( $\text{M} = \text{Aluminum, Chromium}$ ) Catalysts. *J. Catal.* **1989**, *116*, 222.
- (11) Klier, K.; Herman, R. G.; Simmons, G. W.; Nunan, J. G.; Smith, K. J.; Bogdan, C. E.; Himelfarb, P. B. Direct Synthesis of 2-Methyl-1-Propanol/Methanol Fuels and Feedstocks. Final Technical Report DOE/PC/70021-T1-Rev.1, Lehigh University, Bethlehem, PA, 1988.
- (12) Watson, P. R.; Somorjai, G. A. The Hydrogenation of Carbon Monoxide over Rhodium Oxide Surfaces. *J. Catal.* **1981**, *72*, 347.
- (13) Inoue, M.; Miyake, T.; Takegami, Y.; Inui, T. Direct Alcohol Synthesis from Syngas on Ruthenium-Molybdenum-Sodium/Alumina Catalysts: Effects of Physical Properties of Alumina Supports. *Appl. Catal.* **1987**, *29*, 285.
- (14) Anderson, R. B. Nitrided Iron Catalysts for the Fischer-Tropsch Synthesis in the Eighties. *Catal. Rev.-Sci. Eng.* **1980**, *21*, 53.
- (15) Sugier, A.; Freund, E. Primary, Saturated, and Straight Chain Alcohols from Synthesis Gas. U.S. Patent 4,122,110, 1978.
- (16) Quarderer, G. J.; Cochran, K. A. Catalytic Process for Producing Mixed Alcohols from Hydrogen and Carbon Monoxide. European Patent 0,119,609, 1984.
- (17) Stevens, R. R. Alcohols from Synthesis Gas. European Patent 0,172,431, 1986.
- (18) Kinkade, N. E. Alcohols from Carbon Monoxide and Hydrogen Using an Alkali-Molybdenum Sulfide Catalyst. European Patents 0,149,255 and 0,149,256, 1985.

- (19) Xie, Y.; Naasz, B. M.; Somorjai, G. A. Alcohol Synthesis from CO and H<sub>2</sub> over Molybdenum Sulfide. *Appl. Catal.* **1986**, 27, 233.
- (20) Klier, K.; Herman, R. G.; Simmons, G. W.; Lyman, C. E.; Santiesteban, J. G.; Najbar, M.; Bastian, R. Direct Synthesis of Alcohol Fuels over Molybdenum-Based Catalysts. Final Technical Report DOE/PC/80014-T1, Contract No. DE-AC22-85PC80014, Lehigh University, Bethlehem, PA, 1988.
- (21) Tatsumi, T.; Muramatsu, A.; Tominaga, H. Supported Molybdenum Catalysts for Alcohol Synthesis from CO-H<sub>2</sub>. *Appl. Catal.* **1987**, 34, 77.
- (22) Jiang, M.; Bian, G.-Z.; Fu, Y.-L. Effect of the K-Mo Interaction in K-MoO<sub>3</sub>/γ-Al<sub>2</sub>O<sub>3</sub> Catalysts on the Properties for Alcohol Synthesis from Syngas. *J. Catal.* **1994**, 146, 144.
- (23) Lee, J. S.; Kim, S.; Lee, K. H.; Nam, I.-S.; Chung, J. S.; Kim, Y. G.; Woo, H. C. Role of Alkali Promoters in K/MoS<sub>2</sub> Catalysts for CO-H<sub>2</sub> Reactions. *Appl. Catal. A* **1994**, 110, 11.
- (24) Duchet, J. C.; van Oers, E. M.; de Beer, V. H. J.; Prins, R. Carbon-Supported Sulfide Catalysts. *J. Catal.* **1983**, 80, 386.
- (25) Liu, Z.; Li, X.; Close, M. R.; Kugler, E. L.; Petersen, J. L.; Dadyburjor, D. B. Screening of Alkali-Promoted Vapor-Phase-Synthesized Molybdenum Sulfide Catalysts for the Production of Alcohols from Synthesis Gas. *Ind. Eng. Chem. Res.* **1997**, 36, 3085.
- (26) Watson, P. R.; Somorjai, G. A. The Formation of Oxygen-Containing Organic Molecules by the Hydrogenation of Carbon Monoxide over a Lanthanum Rhodate Catalyst. *J. Catal.* **1982**, 74, 282.
- (27) Mross, W. D. Alkali Doping in Heterogeneous Catalysis. *Catal. Rev.—Sci. Eng.* **1983**, 25, 591.
- (28) Ponc, V. Active Centers for Synthesis Gas Reactions. *Catal. Today* **1992**, 12, 227.
- (29) Santiesteban, J. G.; Bogdan, C. E.; Herman, R. G.; Klier, K. Mechanism of C<sub>1</sub>-C<sub>4</sub> Alcohol Synthesis over Alkali/MoS<sub>2</sub> and Alkali/Co/MoS<sub>2</sub> Catalysts. In *Proc. 9th Intern. Congr. Catal.*, Vol. 2, Calgary, Canada; Phillips, M. J., Ternan, M., Eds.; The Chemical Institute of Canada: Ottawa, 1988; p 561.
- (30) Anderson, R. B. *The Fischer-Tropsch Synthesis*; Academic: Orlando, 1984; p 145.
- (31) Tatsumi, T.; Muramatsu, A.; Tominaga, H. Molybdenum Catalysts for Synthesis of Mixed Alcohols from Synthesis Gas. *Sekiyu Gakkaishi (J. Jpn. Petrol. Inst.)* **1992**, 35, 233.
- (32) Conway, M. M.; Murchison, C. B.; Stevens, R. R. Alcohols from Synthesis Gas. (Continuation of European Patents 0,170,973 and 0,172,431). U.S. Patent 4,675,344, 1987.
- (33) Stevens, R. R. Process for Producing Alcohols from Synthesis Gas. U.S. Patent 4,752,622, 1988.
- (34) Murchison, C. B.; Conway, M. M.; Stevens, R. R.; Quaderer, G. J. Mixed Alcohols from Syngas over Moly Catalysts. In *Proc. 9th Intern. Congr. Catal.*, Vol. 2, Calgary, Canada; Phillips, M. J., Ternan, M., Eds.; The Chemical Institute of Canada: Ottawa, 1988; p 626.
- (35) Gunturu, A. K.; Kugler, E. L.; Cropley, J. B.; Dadyburjor, D. B. A Kinetic Model for the Synthesis of High-Molecular-Weight Alcohols over a Sulfided Co-K-Mo/C Catalyst. *Ind. Eng. Chem. Res.* **1998**, 37, 2107.

Received for review February 27, 1998  
 Revised manuscript received July 15, 1998  
 Accepted July 24, 1998

IE980136U